Spontaneous Soliton Formation and Modulational Instability in Bose-Einstein Condensates

L. D. Carr[1] and J. Brand[2]

[1]*Laboratoire Kastler Brossel, Ecole Normale Supérieure, 24 rue Lhomond, 75231 Paris, France*
[2]*Max Planck Institute for the Physics of Complex Systems, Nöthnitzer Straße 38, 01187 Dresden, Germany*

(Received 13 March 2003; published 28 January 2004)

The dynamics of an elongated attractive Bose-Einstein condensate in an axisymmetric harmonic trap is studied. It is shown that density fringes caused by self-interference of the condensate order parameter seed modulational instability. The latter has novel features in contradistinction to the usual homogeneous case known from nonlinear fiber optics. Several open questions in the interpretation of the recent creation of the first matter-wave bright soliton train [K. E. Strecker *et al.*, Nature (London) **417**, 150 (2002).] are addressed. It is shown that primary transverse collapse, followed by secondary collapse induced by soliton-soliton interactions, produces bursts of hot atoms at different time scales.

DOI: 10.1103/PhysRevLett.92.040401 PACS numbers: 03.75.Lm, 05.45.Yv

Solitons are ubiquitous in nature, appearing in systems as diverse as DNA, shallow water, and laser light pulses in nonlinear fiber optics [1]. Modulational instability (MI), an effect well known in the latter context, is the process by which a constant-wave background becomes unstable to sinusoidal modulations because of the presence of a focusing nonlinearity, leading to a pulsed wave, called a bright soliton train [2]. Recently, the first matter-wave bright solitons were created from attractive Bose-Einstein condensates (BEC's) in elongated harmonic traps [3,4]. In the latter experiment, a train of from four to ten solitons was formed; however, unlike the solitons resulting from MI of a uniform initial wave function in a constant potential in one dimension [2], these solitons were apparently stabilized by repulsive soliton-soliton interactions. Moreover, of the $\sim 3 \times 10^5$ initial atoms present when the focusing nonlinearity was turned on, only $\sim 10\%$ survived to form the soliton final state, implying massive collapse. It was suggested [4,5] that MI, in this new context, creates such a repulsively interacting soliton train.

In the following, the MI of a *nonuniform* initial state in the presence of a harmonic potential is studied both analytically and numerically in the context of the mean field of the BEC. The conditions by which the transverse dimensions may bring about *primary collapse,* either of the entire condensate in the radial direction or of individual solitons as they are formed by MI, as well as *secondary collapse* induced by soliton–soliton interactions, are detailed. As a matter-wave bright soliton train is, in fact, a train of self-contained BEC's easily guided and manipulated by electromagnetic fields, it is important to understand how it is made and how it may be kept stable. Moreover, bright solitons, which have already revolutionized the communications industry [1], are, in the context of the BEC, predicted to have applications in atom interferometry and quantum frequency standards [6].

The results of our analysis differ strongly from those of previous studies [2,5]. First, it is shown that self-interference of the order parameter seeds MI at different times and with a steadily decreasing wavelength. This is true for any nonuniform initial density with the exception of a Gaussian. Second, it is shown that the ensuing solitons may have any relative phase and, therefore, may interact both repulsively and attractively. Third, it is shown that both primary and secondary collapse occurs. This leads to the testable experimental prediction of bursts of hot atoms emitted at different time scales and to the conjecture that trajectories of remaining solitons are stabilized by selection, as detailed below.

The 3D nonlinear Schrödinger equation (NLS) or Gross-Pitaevskii equation which describes the mean field of the BEC is written as [7]

$$[-\hbar^2\nabla^2/2m + gN|\Psi|^2 + V(\vec{r})]\Psi = i\hbar\partial_t\Psi, \qquad (1)$$

where $V(\vec{r}) \equiv m(\omega_\rho^2\rho^2 + \omega_z^2 z^2)/2$, $g \equiv 4\pi\hbar^2 a_s/m$, a_s is the s-wave scattering length, m is the atomic mass, N is the number of condensed atoms, the condensate order parameter $\Psi = \Psi(\vec{r}, t)$ has been normalized to one, and axisymmetric confinement has been assumed. Note that for negative scattering length, or attractive nonlinearity, solutions are liable to collapse in certain parameter regimes, as shall be discussed below. In the case of strongly anisotropic confinement, one may adiabatically separate the slow longitudinal from the fast transverse degrees of freedom. The adiabatically varying transverse state obeys a 2D NLS which shows an instability towards collapse. The criterion for stability found by numerical integration of the 2D NLS is

$$\eta \equiv -8\pi a_s N|\psi(z, t)|^2 < 11.7, \qquad (2)$$

where $N|\psi(z, t)|^2$ is the local axial line density of the condensate [8]. If adiabaticity is violated, collapse can also happen at weaker nonlinearity due to transverse oscillations on a time scale π/ω_ρ [9]. When the longitudinal dynamics is significantly slower than this time scale, the adiabatic separation is valid. If, additionally, the transverse nonlinearity is weak, i.e., $|\eta| \ll 1$, the

longitudinal equation reduces to the quasi-1D NLS

$$[-\hbar^2\partial_z^2/2m + g_{1D}N|\psi|^2 + m\omega_z^2 z^2/2]\psi = i\hbar\partial_t\psi, \quad (3)$$

where $g_{1D} \equiv 2a_s\omega_\rho\hbar$ is the quasi-1D coupling constant [10], provided $l_\rho \gg |a|$ [11], with $l_\rho \equiv \sqrt{\hbar/(m\omega_\rho)}$.

In order to understand the mechanism of MI for a nonuniform initial density profile and in the presence of a nonconstant potential, it is necessary to briefly review MI in the uniform case, which is well known from fiber optics [2]. A linear response analysis reveals that, for attractive nonlinearity, a small sinusoidal modulation of a uniform state ψ_0 with wave number k grows exponentially at a rate γ given by

$$\gamma^2 = -\frac{\hbar^2}{4m^2}\left[k^2 - \frac{2Nm|g_{1D}|\,|\psi_0|^2}{\hbar^2}\right]^2 + \frac{|\psi_0|^4N^2|g_{1D}|^2}{\hbar^2}. \quad (4)$$

The maximum growth rate $\gamma_{mg} = 2\omega_\rho|a_s|N|\psi_0|^2$ is obtained at wave number $k_{mg} = 1/\xi$, where $\xi = l_\rho/\sqrt{4|a_s|\,N\,|\psi_0|^2}$ is the effective 1D healing length of the condensate [12]. Note that $N|\psi_0|^2$ is the line density of the condensate. Growth occurs only if $\gamma^2 > 0$, which implies $0 < k < k_{max} = \sqrt{2}k_{mg}$. This means that nonlinear focusing can be seeded only by modulations of sufficiently long wavelength and is fastest at the length scale of $2\pi\xi$.

For *nonuniform* initial density profiles, self-interference fringes in the order parameter can provide the necessary seed. To understand this phenomenon, it is instructive to first consider the development of the wave function for the ideal gas ($a_s = 0$). As a model, we shall consider the case of an initial state $\psi(z, 0)$ which is a rectangular function of height ψ_0 and width L centered at the origin. Recall that the Feynman propagator which determines the evolution of the wave function in the *linear* Schrödinger equation is defined by $\psi(z, t) = \int dz' G(z, t; z', 0)\psi(z', 0)$. In the case of a harmonic potential, G may be determined exactly by semiclassical methods to be [13,14]

$$G = \frac{\exp\{i(z^2 - 2zz'/\cos\tau + z'^2)/(2l_z^2\tan\tau)\}}{l_z\sqrt{2\pi i|\sin\tau|}}, \quad (5)$$

where $\tau = \omega_z t$ and $l_z \equiv \sqrt{\hbar/(m\omega_z)}$ is the axial harmonic oscillator length. This gives an analytic expression for the evolution of the order parameter, which may be more easily understood in the limit $\omega_z t \ll 1$:

$$\frac{|\psi|^2}{|\psi_0|^2} \simeq 1 + \sqrt{\frac{8l_z^2\omega_z t}{\pi}}\left[\frac{\sin(k_+z + \delta - \frac{\pi}{4})}{L + 2z} + \frac{\sin(k_-z + \delta - \frac{\pi}{4})}{L - 2z}\right] + \frac{4l_z^2\omega_z t}{\pi}\left\{\frac{L^2 + 4z^2}{(L + 2z)^2(L - 2z)^2} + \frac{\cos[(k_+ - k_-)z]}{(L + 2z)(L - 2z)}\right\} + \frac{1}{2}\omega_z^2t^2 + \mathcal{O}[(\omega_z t)^{5/2}], \quad (6)$$

$$\mathrm{Arg}(\psi) \simeq \sqrt{\frac{2l_z^2\omega_z t}{\pi}}\left[\frac{\sin(k_+z + \delta + \frac{\pi}{4})}{L + 2z} + \frac{\sin(k_-z + \delta + \frac{\pi}{4})}{L - 2z}\right] + \frac{l_z^2\omega_z t}{\pi}\left\{-\frac{z^2\pi}{l_z^4} + \frac{\cos[2(k_+z + \delta)]}{(L + 2z)^2} + \frac{\cos[2(k_-z + \delta)]}{(L - 2z)^2} + \frac{\cos[(k_+ + k_-)z + 2\delta]}{(L + 2z)(L - 2z)}\right\} + \mathcal{O}[(\omega_z t)^{3/2}], \quad (7)$$

$$k_\pm \equiv \frac{\sec(\omega_z t)z \pm L}{2l_z^2\sin(\omega_z t)}, \qquad \delta \equiv \frac{L^2\cot(\omega_z t)}{8l_z^2}, \qquad |z| < \frac{L}{2}, \quad (8)$$

Figures 1(b) and 2(b) show the density and phase structures given by Eqs. (6)–(8), respectively. Note that the above expansions converge very slowly as $|z| \to L/2$ where the initial wave function is discontinuous.

The above expressions for the evolution of the phase and density of the wave function may be understood as follows. All *trigonometric* terms represent quantum self-interference and produce fringes which seed MI. The wave number $k_\pm$ is dependent on both time and position; the wavelength is longer and the amplitude of oscillations higher at the edges of the box than in the center, and the overall wavelength increases as a function of time. As these interference terms are to linear order independent of ω_z (since $l_z^2\omega_z = \hbar/m$), they must result solely from the nonuniform initial density profile. One may also understand this result by observing that Eq. (5) is, to order $\omega_z t$, identical with the free space Feynman propagator in one dimension. In contrast, the *nontrigonometric* terms are caused by the harmonic potential: in Eq. (6) they lead to a monotonic increase in the mean density, where the order $(\omega_z t)^2$ term is independent of position; and in Eq. (7) they develop the overall phase profile harmonically. The development of the density and phase of the wave function for the geometry of Ref. [4] of $L \sim 10l_z$ is shown in Figs. 1 and 2.

MI of a nonuniform initial state, both with and without an additional harmonic potential, may be understood in light of the above considerations. In Fig. 3 is shown the numerical evolution of the axial line density $N|\psi|^2$ in Eq. (3) for the parameters of Strecker *et al.* [4] and our model of an initial square function. The fringes produced by self-interference of the condensate order parameter ψ attain the critical wavelength for MI of $\sqrt{2}\pi\xi$ first at the edges of the cloud, as shown in Figs. 1 and 2. In Fig. 3 one notes that the solitons are therefore formed last in the center of the trap. In this latter stage they are also formed closer together, as, because of both the harmonic

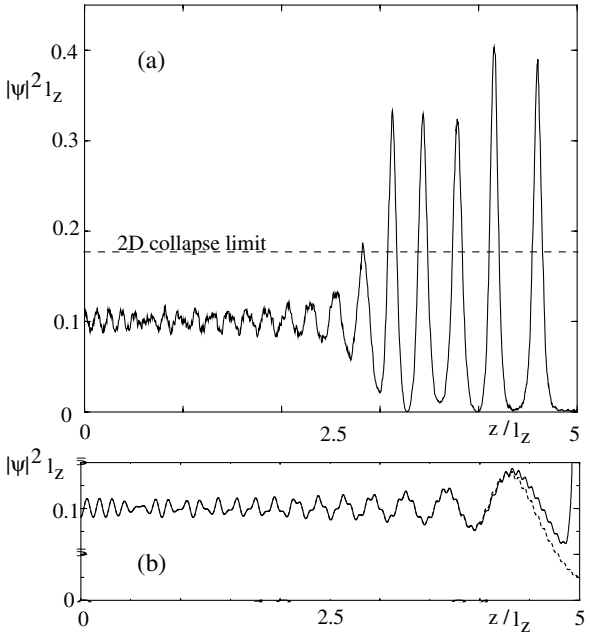

FIG. 1. Shown is the right half of the axial density of a BEC in a harmonic potential, as determined by (a) numerical solution of the *nonlinear* Schrödinger equation, and (b) analytical solution of the *linear* Schrödinger equation (dashed line: exact; solid line: approximate), at $t = 0.016 \times 2\pi/\omega_\rho$, after 1D evolution from an initial box state of length $L/l_z = 10$ centered at the origin. The formation of solitons first at the edge of the condensate in (a) results from the longer wavelength of the linear fringes, as seen in (b), since MI takes place at a wavelength $\sim 2\pi\xi = 0.43 l_z$ in this simulation, using the parameters of Strecker *et al.* [4,15].

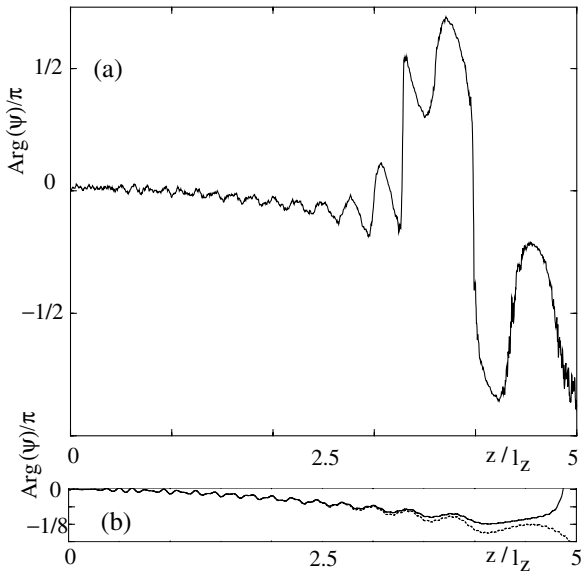

FIG. 2. Shown is the phase of the order parameter corresponding to Figs. 1(a) and 1(b). The phase difference $\Delta\phi$ between solitons may be seen by comparing to the large density peaks of Fig. 1(a): $\Delta\phi$ is highly sensitive to the nonlinearity, and may take on arbitrary values between 0 and 2π, in contrast to the usual case of MI in fiber optics, where it is restricted to 0. At later stages in the simulation, the relative phases drift as the solitons decouple.

potential [see Eq. (7)] and the global focusing effect of the nonlinearity, the axial density has increased, and $\xi \propto |\psi|^{-1}$. Note that, although the early phase structure in Fig. 2 depends only weakly on the harmonic potential, in later stages of evolution the trap affects the phase strongly.

One may ask if the seed fringes are caused by the sharpness of the square function edges in our model. In the particular case $\omega_z t = \pi/4$, Eq. (5) takes the form of a Fourier transform, $\psi(z, t) \propto \int dz' \exp(-izz'/l_z^2)\psi(z', 0)$. Thus, it is immediately apparent that all initial wave functions with the exception of a Gaussian must develop fringes. In order to test the full time development for an experimentally relevant initial density, a Thomas-Fermi profile of harmonic trapping [7] with $\psi \propto \sqrt{1 - (2z/L)^2}$ for $|z| < L/2$ and $\psi = 0$ for $|z| \geq L/2$ was also studied and was found to have qualitatively the same evolution in the linear Schrödinger equation, i.e., fringes of longer wavelength towards the outer edges of the density profile and an overall increase in wavelength with time. The nonlinear evolution also shows the same qualitative behavior as Fig. 3, with solitons forming spontaneously first near the edges and later toward the center.

Besides the initial linear density fringes and nonlinear MI, the condensate can undergo primary transverse collapse on a time scale π/ω_ρ, according to Eq. (2). In the Strecker experiment, a rough estimate assuming a constant initial density yields $\eta \approx 6.3$. In fact, η will exceed this value locally due to the slanted initial profile produced by creating the BEC on one side of the trap [4], and transverse collapse is likely to occur on the higher density side of the profile before MI develops. However, even for a uniform initial state, the critical value of η is reached during soliton formation as indicated in Fig. 2. Note that the center of mass of the BEC, created at the side of the trap, trivially oscillates with the harmonic oscillator frequency and decouples completely [16] from the relative motion, the latter of which is analyzed in this work.

After the soliton train has spontaneously formed, even if transverse collapse is avoided, individual solitons can undergo primary 3D collapse, which dominates over transverse instabilities. The static condition for three-dimensional soliton stability in the absence of longitudinal confinement is given numerically by [10]

$$N_{\text{crit}}|a_s|/l_\rho = 0.627\ldots. \tag{9}$$

Dynamical effects, as, for example, breathing of the soliton, can lower this condition further. In light of a recent experiment on a single matter-wave bright soliton [3], it is anticipated that such a three-dimensional collapse will eject the excess number of atoms, leaving behind a solitonic core which is near the limit of Eq. (9). In the simulation of Figs. 1–3, the 26 solitons formed carry an average of $\approx 1.9 N_{\text{crit}}$ atoms where $N_{\text{crit}} \approx 6100$ for the parameters of the Strecker experiment. These results are supported by a coarse estimate based on

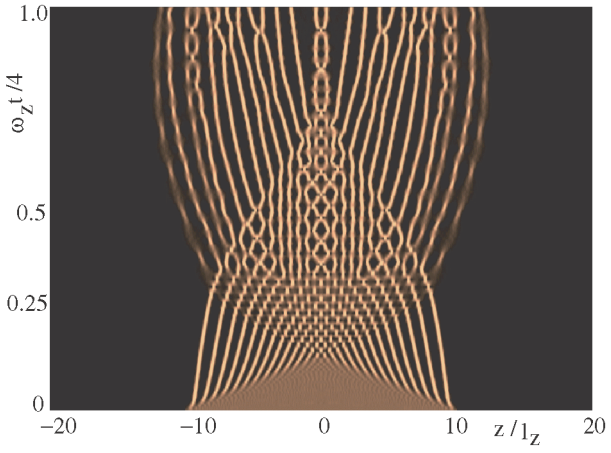

FIG. 3 (color online). Shown is the 1D evolution of the axial density of an elongated Bose-Einstein condensate when the interactions are suddenly tuned negative, starting from a box-like initial state. Here the parameters of the Strecker experiment [4] are used. At early times, small fringes develop as the time slice of Fig. 1 clearly shows; once the MI is seeded, the nonlinearity focuses the fringes to produce solitons, the leading edge of which is seen at the bottom of the figure as a wide triangle shape. Lines visible above this edge are solitons. Their complicated interaction pattern clearly shows many examples of both attractive and repulsive soliton interactions.

Eq. (4), which predicts formation of 22 solitons, and by simulations of the 3D NLS analogous to the one of Figs. 1–3, which shows primary collapse immediately after formation of the first solitons (not shown).

Finally, the coherent overlap of solitons, not themselves subject to two- or three-dimensional collapse, can cause secondary collapse. The dynamics of binary soliton interactions are determined by their relative phase $\Delta\phi$ and amplitude ΔA [17]. For $-\pi/2 < \Delta\phi < \pi/2$ they attract each other and exchange mass. Consequently, they can undergo collapse if, during their interaction, they temporarily violate Eq. (9). For $\pi/2 < \Delta\phi < 3\pi/2$ and $\Delta A = 0$ the interaction is repulsive and there is no mass exchange; the solitons are stable against secondary collapse induced by interactions. However, for $\Delta A \neq 0$ the relative phase cycles periodically which, if it crosses over into the regime $-\pi/2 < \Delta\phi < \pi/2$, can again cause collapse. Based on the above and the experiment of Ref. [3], we conject that, in the Strecker experiment, collisions of solitons close to N_{crit} led, by several stages of secondary collapse, to a final configuration of a small number of solitons with stable trajectories. We emphasize that these results differ from those found in Ref. [5], where it was suggested that the phase difference $\Delta\phi$ between adjacent solitons originates from quantum fluctuations and is restricted to values close to π, thus stabilizing their trajectories. MI of a nonuniform initial state already produces arbitrary $\Delta\phi$ in a mean-field model. We conject that it is the secondary collapse processes which determine a stable trajectory of solitons in the final state with $\pi/2 < \Delta\phi < 3\pi/2$.

The 2D and 3D collapse processes of Eqs. (2) and (9) occur on different time scales. It is likely that both processes contributed to the ~90% initial atom loss in the Strecker experiment; a measurement of the time dependence of the atomic mass ejected from the trap during the initial stages of soliton train formation may be able to determine if one or both were dominant. For the experimental parameters, based on the collapse conditions and Fig. 3, primary transverse collapse occurs on a time scale of $\lesssim 1.7$ ms, primary 3D collapse occurs between 1.5 and 10 ms, and secondary collapse occurs at $\gtrsim 10$ ms.

In conclusion, the phenomenon of MI has been analyzed in the case of a nonuniform initial state in the nonlinear Schrödinger equation with a harmonic potential. It was shown that linear density fringes, the length scale of which depends on both space and time, seed the nonlinear instability. Primary transverse collapse, primary three-dimensional soliton collapse, and secondary three-dimensional collapse due to soliton binary interactions were discussed, and all were predicted to have played a role in the Strecker experiment [4].

We thank Y. Castin, R. Hulet, and G. Shlyapnikov for useful discussions. L. D. C. was supported by NSF Grant No. MPS-DRF 0104447. LKB is a unit of ENS and of Université Paris 6 associated with CNRS. We thank the ECT* (Trento) and MPIPKS (Dresden) for hosting us during various stages of this work.

[1] G. P. Agrawal, *Nonlinear Fiber Optics* (Academic Press, San Diego, 1995), 2nd ed.
[2] A. Hasegawa and W. F. Brinkman, IEEE J. Quantum Electron. **16**, 694 (1980).
[3] L. Khaykovich *et al.*, Science **296**, 1290 (2002).
[4] K. E. Strecker *et al.*, Nature (London) **417**, 150 (2002).
[5] U. Al Khawaja *et al.*, Phys. Rev. Lett. **89**, 200404 (2002).
[6] Yu. V. Rozhdestvenskii, N. N. Rozanov, and V. A. Smirnov, JETP Lett. **76**, 370 (2002).
[7] F. Dalfovo, S. Giorgini, L. P. Pitaevskii, and S. Stringari, Rev. Mod. Phys. **71**, 463 (1999).
[8] M. I. Weinstein, Commun. Math. Phys. **87**, 567 (1983); A. Gammal *et al.*, Phys. Lett. A **267**, 305 (2000).
[9] L. P. Pitaevskii, Phys. Lett. A **221**, 14 (1996).
[10] L. D. Carr and Y. Castin, Phys. Rev. A **66**, 063602 (2002).
[11] M. Olshanii, Phys. Rev. Lett. **81**, 938 (1998).
[12] The growth rate may also be calculated numerically, as in N. N. Akhmediev *et al.*, Opt. Lett. **17**, 393 (1992).
[13] E. P. Storey, Ph.D. thesis, L'École Normale Supérieure, 1996.
[14] Up to a global phase $\nu(t)$, which has no physical significance for the observables, since the important quantity for soliton interactions is relative phase.
[15] The parameters used are $N = 3 \times 10^5$, $\omega_z = 2\pi \times 3$ Hz, $\omega_\rho = 2\pi \times 600$ Hz, and $a_s = -3a_0$.
[16] J. J. García-Ripoll, V. M. Pérez-García, and V. Vekslerchik, Phys. Rev. E **64**, 056602 (2001).
[17] J. P. Gordon, Opt. Lett. **8**, 596 (1983).